Bioorganic & Medicinal Chemistry Letters 23 (2013) 2996–3000

Contents lists available at SciVerse ScienceDirect

Bioorganic & Medicinal Chemistry Letters

journal homepage: www.elsevier.com/locate/bmcl

Discovery of ML326: The first sub-micromolar, selective M_5 PAM

Patrick R. Gentry [b,c,d], Thomas M. Bridges [b,c], Atin Lamsal [e], Paige N. Vinson [b,c], Emery Smith [e], Peter Chase [e], Peter S. Hodder [e,f], Julie L. Engers [b,c], Colleen M. Niswender [a,b,c], J. Scott Daniels [a,b,c], P. Jeffrey Conn [a,b,c], Michael R. Wood [a,b,c,d], Craig W. Lindsley [a,b,c,d,*]

[a] Department of Pharmacology, Vanderbilt University Medical Center, Nashville, TN 37232, USA
[b] Vanderbilt Center for Neuroscience Drug Discovery, Vanderbilt University Medical Center, Nashville, TN 37232, USA
[c] Vanderbilt Specialized Chemistry Center for Probe Development (MLPCN), Nashville, TN 37232, USA
[d] Department of Chemistry, Vanderbilt University, Nashville, TN 37232, USA
[e] Scripps Research Institute Molecular Screening Center, Lead Identification Division, Translational Research Institute, 130 Scripps Way, Jupiter, FL 33458, USA
[f] Department of Molecular Therapeutics, Scripps Florida, 130 Scripps Way, Jupiter, FL 33458, USA

ARTICLE INFO

Article history:
Received 21 January 2013
Revised 28 February 2013
Accepted 7 March 2013
Available online 16 March 2013

Keywords:
Muscarinic acetylcholine receptors
M_5
Positive allosteric modulator (PAM)
ML326

ABSTRACT

This Letter describes the further chemical optimization of the M_5 PAM MLPCN probes ML129 and ML172. A multi-dimensional iterative parallel synthesis effort quickly explored isatin replacements and a number of southern heterobiaryl variations with no improvement over ML129 and ML172. An HTS campaign identified several weak M_5 PAMs (M_5 EC_{50} >10 μM) with a structurally related isatin core that possessed a southern phenethyl ether linkage. While SAR within the HTS series was very shallow and unable to be optimized, grafting the phenethyl ether linkage onto the ML129/ML172 cores led to the first sub-micromolar M_5 PAM, ML326 (VU0467903), (human and rat M_5 EC_{50}s of 409 nM and 500 nM, respectively) with excellent mAChR selectivity (M_1–M_4 EC_{50}s >30 μM) and a robust 20-fold leftward shift of the ACh CRC.

There are five muscarinic acetylcholine receptor (mAChR) subtypes (M_1–M_5) widely expressed in both the central nervous system (CNS) and periphery of mammals.[1–5] These receptors, whose endogenous agonist is acetylcholine (ACh), play critical roles in regulating a variety of diverse physiological processes. Within the CNS, the M_1, M_4 and M_5 subtypes are believed to be the most important with respect to normal neuronal functioning.[1–5] Of these three, M_5 is the least studied as a combined result of its lower expression levels[6] (<2% of total muscarinic receptor population within the brain) and, until recently, a near absence of highly selective M_5 receptor ligands. Much of our current understanding surrounding the function of M_5 has come from M_5 receptor localization, M_5 knock-out mice[7] and experiments conducted with non-selective muscarinic ligands.[8] It is intriguing to note that the M_5 receptor is the only muscarinic receptor observed the substantia nigra pars compacta (based on mRNA detection),[9,10] leading to the prediction that M_5 functions in addiction/reward mechanisms. This hypothesis was supported in man through the clinically observed correlation between a specific M_5 gene mutation and an increase in cigarette consumption (+27%), as well as, an increased risk for cannabis dependence (+290%).[11] Additionally, M_5 receptors have been localized on the cerebrovascular system and shown to be critical in the ACh-induced dilation necessary for normal blood perfusion.[12] In a broader sense, M_5 KO mice show decreased prepulse inhibition,[13] CNS neuronal abnormalities and cognitive deficits,[14] thus supporting the potential for M_5 ligands in the treatment of numerous CNS disorders including schizophrenia, Alzheimer's disease, ischemia and migraine.[1–5]

To date, few M_5 PAMs have been reported,[15–17] and none of these display the potency and efficacy necessary to definitively probe the role of selective M_5 activation (Fig. 1); therefore, in this Letter, we detail the further optimization of these ligand, and the discovery of the first submicromolar and selective M_5 PAMs.

Within the isatin scaffold, alternate substitution afforded a highly selective M_1 PAM, ML137, **4**.[18] We recently reported on a number of replacements (tertiary hydroxyls and spirocyclic replacements, etc.) for the isatin moiety that maintained M_1 PAM activity (Fig. 2).[19,20] Therefore, our optimization plan for ML129 consisted of evaluating both spirocyclic and other replacements for the isatin moiety, while continuing to investigate alternatives for the southern *p*-OMe benzyl motif in an effort to improve M_5 PAM potency to below 1 μM (Fig. 3).

First, we explored alternatives to the 5-OCF_3 moiety on the isatin core, and despite evaluating other positions and alternate functionalities, all were devoid of M_5 PAM activity. Employing the chemistry previously reported for analogs **5** of ML137,[19] we prepared the corresponding 3° hydroxyl and dioxalane analogs of

* Corresponding author.
E-mail address: craig.lindsley@vanderbilt.edu (C.W. Lindsley).

0960-894X/$ - see front matter © 2013 Elsevier Ltd. All rights reserved.
http://dx.doi.org/10.1016/j.bmcl.2013.03.032

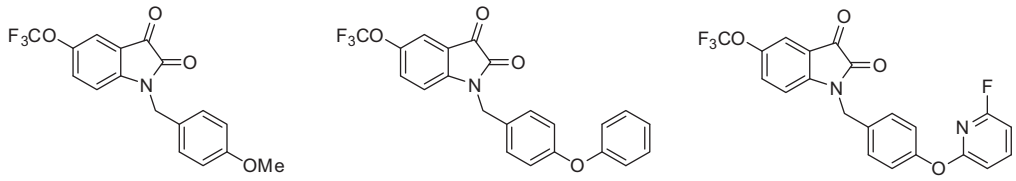

1, **ML129**
hM_5 EC_{50} = 1.1 μM (91% ACh_{max})
hM_5 ACh fold shift (@30 μM) = 14-fold
hM_1 - hM_4 EC_{50} > 30 μM

2, **ML172**
hM_5 EC_{50} = 1.9 μM (75% ACh_{max})
hM_5 ACh fold shift (@30 μM) = 5-fold
hM_1 - hM_4 EC_{50} >> 30 μM

3, **VU0414747**
hM_5 EC_{50} = 1.5 μM (62% ACh_{max})
hM_5 ACh fold shift (@30 μM) = 6-fold
hM_1 - hM_4 EC_{50} >> 30 μM

Figure 1. Structures and activities of the reported M_5 PAMs **1**–**3**. All three were derived from a *pan*-M_1, M_3, M_5-PAM that afforded both M_1 selective PAMs and, by virtue of the 5-OCF_3 moiety, M_5 selective PAMs.

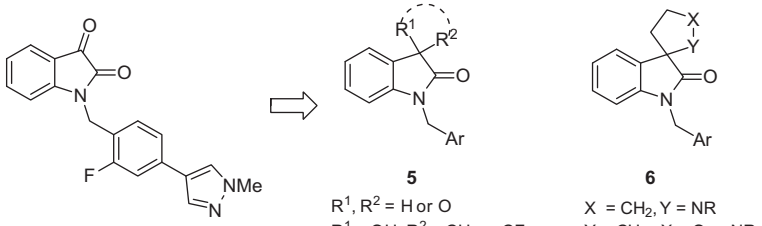

4, **ML137**
hM_1 EC_{50} = 0.6 μM (45% ACh_{max})
hM_2 - hM_5 EC_{50} > 30 μM

5
R^1, R^2 = H or O
R^1 = OH, R^2 = CH_3 or CF_3

6
X = CH_2, Y = NR
Y = CH_2, X = O or NR

Figure 2. Structures and activities of the reported M_1 PAMs **4**–**6**. Mulitple productive replacements (tertiary hydroxyls, dioxalanes and spiro furans/pyrroles) were identified for the isatin moiety of ML137 that maintained selective M_1 PAM activity.

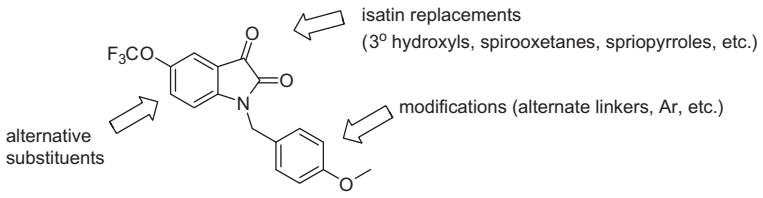

1, ML 129
hM_5 EC_{50} = 1.1 μM (91% ACh_{max})
hM_5 ACh fold shift (@30 μM) = 14-fold
hM_1 - hM_4 EC_{50} > 30 μM

Figure 3. Multi-dimenisional chemical optimization plan for ML129 (**1**).

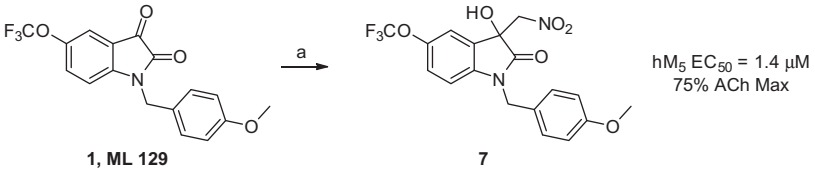

1, ML 129 **7**

hM_5 EC_{50} = 1.4 μM
75% ACh Max

Scheme 1. Synthesis of 3° hydroxyl analog **7**. Reagents and conditions: (a) DABCO, nitromethane (neat), 100%.

ML129, and while there was a slight elevation in the ACh max, all of the analogs were >10 μM as M_5 PAMs, indicating a disconnect in the SAR between M_1 and M_5. We next explored novel 3° hydroxyl analogs with diverse functionalities, which proved to be more productive. Treatment of ML129 with DABCO in nitromethane afforded the 3° alcohol **7** in quantitative yield (Scheme 1);[21] importantly, **7** was of comparable potency and efficacy to ML129 (M_5 EC_{50} = 1.4 μM, 75% ACh Max), but the nitro moiety was not attractive as an in vivo probe.

This led us to explore other 3° alcohols possessing heterocycles, and most notably pyridines. Here, we employed two routes to survey pyridyl analogs **8** and pyridyl methyl homologs **11** (Scheme 2). Again, utilizing ML129 as starting material, exposure to a functionalized pyridyl boronic acid **9** under $Cu(OTf)_2$ catalysis, affords analogs **8** in 25–70% yields.[22] We also employed direct lithiation/addition in some instances.[23] The homologated congeners **11** were easily accessed following the Li protocol,[24] employing picolines under Bronsted acid catalysis. SAR again proved shallow, with all

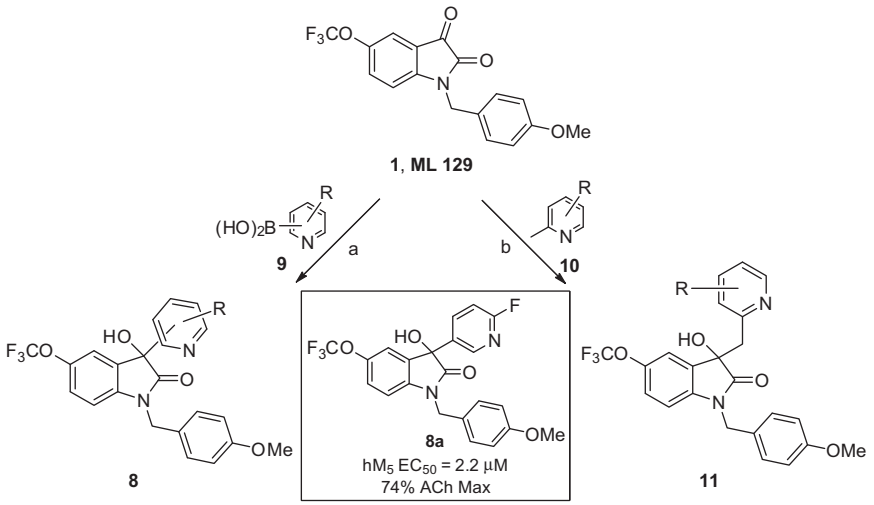

Scheme 2. Synthesis of pyridyl-based 3° hydroxyl analogs **8** and **11**. Reagents and conditions: (a) $Cu(OTf)_2$, 1,10-phenathroline, LiOH, DCE, reflux, 48 h, 5–45%; (b) TfOH, dioxane, 180 °C, mw, 45 min, 22–74%.

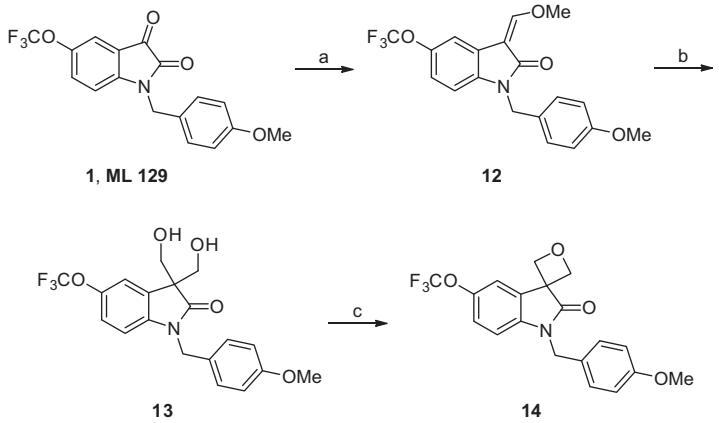

Scheme 3. Synthesis of a spiro-oxetane analog **14**. Reagents and conditions: (a) methyl methoxyphosphonium bromide, LDA, THF, −78 °C to rt, 70%; (b) PTSA, aq formaldehyde, Na_2CO_3, THF: H_2O, rt, 82%; (c) Tf_2O, lutidine, DCM, −78 °C to rt, 6%.

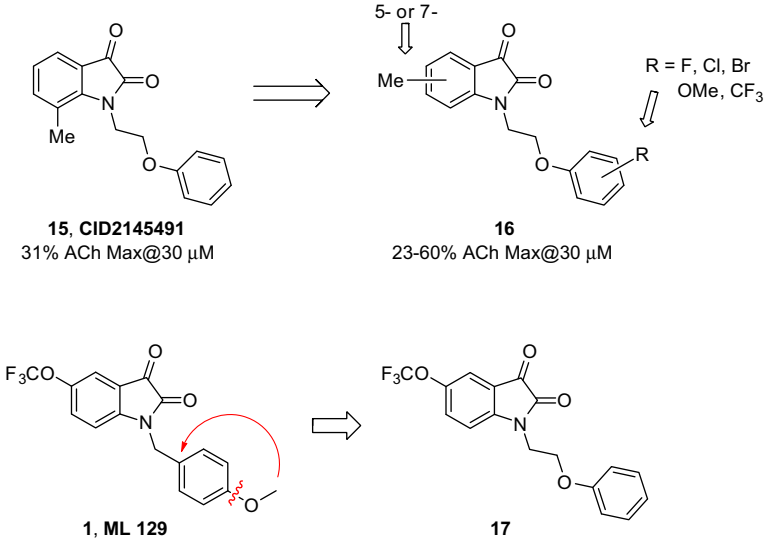

Figure 4. M_5 Triple-add HTS PAM screening hit **15** and related analogs **16**. Could juxtaposition of ML129 into **17** afford an improved M_5 PAM?

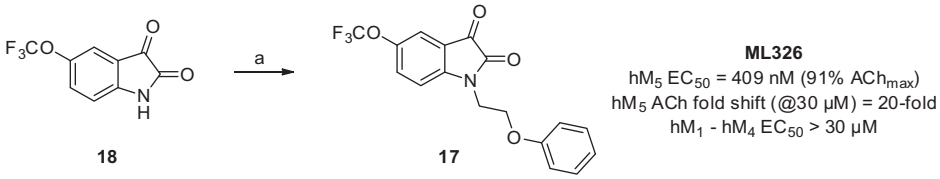

Scheme 4. Synthesis of phenethyl ether analog **17** (ML326). Reagents and conditions: (a) (2-bromoethoxy)benzene, K_2CO_3, KI, ACN, mw, 160 °C, 10 min, 82%.

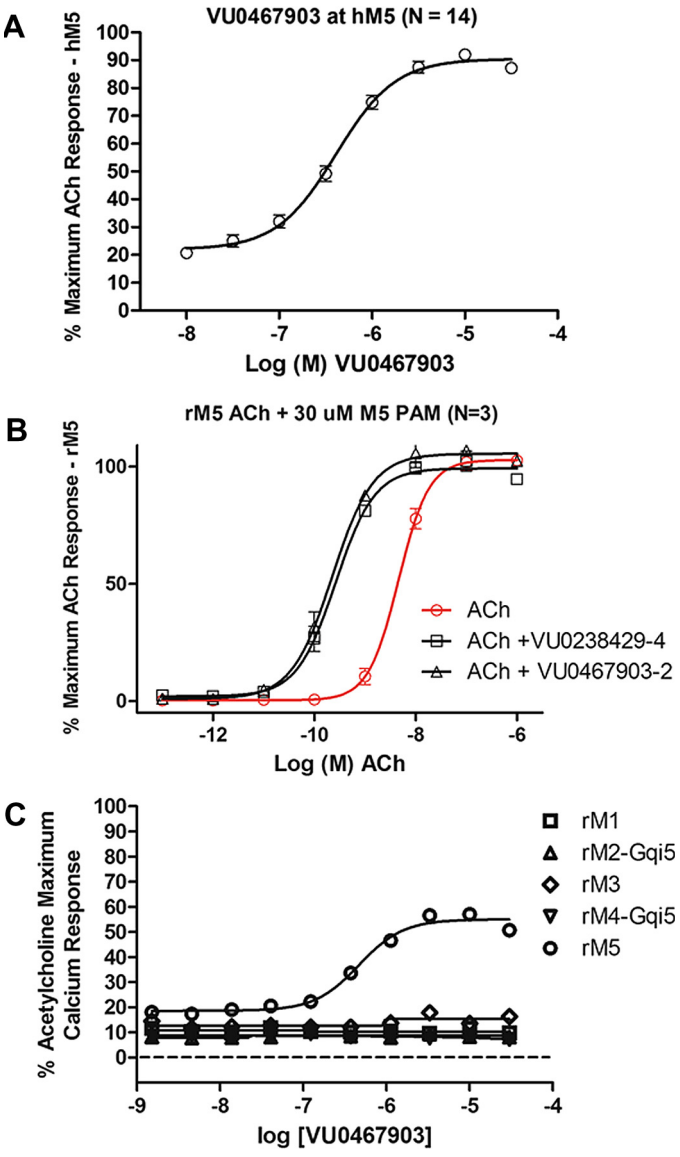

Figure 5. In vitro pharmacological characterization of **17** (VU0467903, ML326). (A) M_5 PAM concentration-response-curve (CRC) afforded an EC_{50} of 409 nM, 91% ACh Max; (B) rat M_5 fold-shift assay with **1** (VU0238429, ML129) and **17**, demonstrating a robust 20-fold shift (human fold-shift data is the same). ACh EC_{50} = 4.58 nM, pEC_{50} = 8.34 ± 0.04, ACh + 429 EC_{50} = 263.4 pM, pEC_{50} = 9.58 ± 0.06, ACh + 903 EC_{50} = 225.4 pM, pEC_{50} = 9.65 ± 0.06; (C) rat mAChR selectivity data with **17**, indicating >30 μM versus M_1–M_4 (human data is the same).

analogs **11** showing no activity as M_5 PAMs; however, one of the 3-pyridyl-based 3° hydroxyls **8a** proved to be a moderately active M_5 PAM (M_5 EC_{50} = 2.2 μM, 74% ACh Max), but SAR was steep.[3]

We therefore elected to introduce a more subtle variant of the istain carbonyl in the form of a spiro-oxetane, and evaluate this carbonyl isostere for M_5 activity (Scheme 3). A Wittig reaction with

Table 1
Structure and activities of analogs 19

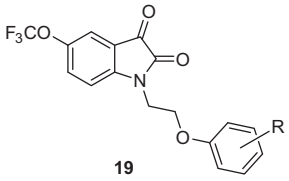

19

Compd	R	M_5EC_{50} (μm)	pEC 50 ± SEM	%ACh Max
ML326	H	0.41	6.39±0.04	91±1.6
19a	4-OPh	1.05	5.98±0.04	93±1.9
19b	4-Cl	0.45	6.35±0.04	92±1.7
19c	4-OMe	0.59	6.23±0.04	89±1.7
19d	3-Me	0.53	6.28±0.03	91±1.3

All values are the average of three independent experiments.

ML129 provided **12**, which was smoothly converted into the diol **13** in 57% overall yield. Mono-triflation of **13** and nucelophilic displacement proceeded in low yield (~6%) to the spioroxetane **14**.[25] Interestingly, **14** was inactive as an M_5 PAM, and only afforded a marginal base-line increase in the ACh Max.

Other modifications, such as spiro-pyrrolidines and dioxalanes, which were well tolerated for M_1 PAM activity in the ML137 series,[19,20] were uniformly inactive on the ML129 scaffold. Clearly, SAR was steep and did not cross-over between M_1 and M_5. Moreover, despite the synthesis and screening of hundreds of analogs of ML129, surveying multiple regions, we were unable to develop a submicromolar M_5 PAM.

At this point, we pursued a new high throughput screen (HTS) for M_5 run in triple-add mode performed on the MLPCN screening deck (~360,000 compounds, PubChem AID 624103).

Early in the process, and prior to official 'hit' confirmation (Fig. 4), we noticed a structurally related, weak single-point (31% at 3 μM) hit, CID2145491 (**15**). This 'hit' possessed a phenethyl ether linkage, a moiety we had not yet explored on the ML129 core, and we were very surprised to find an isatin core without the 5-OCF_3 moiety, and a 7-methyl group)[15] with activity at M_5. We then reviewed the preliminary HTS data, and found a number of related compounds **16** with diverse functionality on the phenyl ring of the phenethyl ether, as well as either a 5- or 7-methyl group on the isatin core with weak M_5 activity (23–60% ACh max at 30 μM). Based on these data, we immediately questioned if the juxtaposition of ML129 with **15**, leading to analog **17** would lead to an improved M_5 PAM.

To evaluate this possibility, we prepared **17** by alkylating the 5-OCF_3 isatin **18** with commercial (2-bromoethyoxy) benzene under microwave-assisted conditions in 82% yield (Scheme 4).[26]

Gratifyingly, this structural modification led to one of the most potent M_5 PAM we have ever identified. Compound **17** (VU0467903), later declared an MLPCN probe and given the designation ML326, was a potent M_5 PAM (Fig. 5) on both human (EC_{50} = 409 nM, 91% ACh Max, pEC 50 = 6.39 ± 0.04) and rat M_5 (EC_{50} = 500 nM, 59% ACh Max). In fold-shift assays, ML326 afforded a robust 20-fold leftward shift of the ACh CRC, and was found to

highly selective versus M_1–M_4 (EC_{50}s >30 μM). Very encouraged by the initial in vitro potency and selectivity profile for ML326 we prepared gram quantities and set about characterizing it through our in-house tier 1 DMPK assays (PPB, rat/human microsomal stability with predicted intrinsic clearance, P_{450} inhibition, rat brain homogenate binding, etc.) and single dose PK/CNS exposure in rat. Many of these experiments were initiated in parallel, including the collection of rat plasma/brain samples; however we encountered insurmountable LCMS/MS analytical quantization issues due to poor ionization of ML326 using ESI, APPI, and APCI ionization probes, which prevented the determination of routine tier 1 DMPK parameters and in vivo rat exposure. Alternative methods including chemical derivatization and UV absorbance also failed to provide the requisite sensitivity for detection of ML326 thus preventing the completion of numerous studies. However, we were able to assess that ML326 had relatively clean CYP and ancillary pharmacology profiles.

Based on this promising data, we prepared other analogs **19** (Table 1) with substituents in the phenyl ring of **17**, following the route depicted in Scheme 4. While this afforded a number of potent and selective M_5 PAMs, they all suffered from the same poor ionization profiles which precluded extensive DMPK profiling. Based on the ionization issue and relatively flat SAR, this series is no longer the subject of chemical optimization.

In summary, further elaboration of the ML129 M_5 PAM structure has been explored, and SAR was particularly steep. Insight from a weak M_5 PAM HTS hit led to the hybridization with ML129 to afford ML326 (VU0467903), the first highly selective (>30 μM versus M_1–M_4) and sub-micromolar (human (EC_{50} = 409 nM, 91% ACh Max) and rat M_5 (EC_{50} = 500 nM, 59% ACh Max)) M_5 PAM. Interestingly, the preliminary HTS hits that inspired the structural modifications to ML129, leading to ML326 did not confirm upon re-order and full CRC. Finally, the poor ionization of ML326 precluded in-depth DMPK profiling; however, ML326 is a valuable in vitro probe and is serving as an important probe in electrophysiology studies, which will be reported shortly.

Acknowledgments

The authors thank the NIH (U54MH084659) and William K. Warren, Jr. who funded the William K. Warren, Jr. Chair in Medicine (to C.W.L.). Vanderbilt University is a Specialized Chemistry Center within the MLPCN and all the ML# probes are freely available upon request. Scripps was supported by the National Institute of Health Molecular Library Probe Production Center grant U54 MH084512. We thank Lina DeLuca (Lead Identification Division, Scripps Florida) for compound management.

References and notes

1. Bonner, T. I.; Buckley, N. J.; Young, A. C.; Brann, M. R. *Science* **1987**, *237*, 527.
2. Dencker, D.; Thomsen, M.; Wörtwein, G.; Weikop, P.; Cui, Y.; Jeon, J.; Wess, J.; Fink-Jensen, A. *ACS Chem. Neurosci.* **2012**, *3*, 80.
3. Melancon, B. J.; Hopkins, C. R.; Wood, M. R.; Emmitte, K. A.; Niswender, C. M.; Christopoulos, A.; Conn, P. J.; Lindsley, C. W. *J. Med. Chem.* **2012**, *55*, 1445.
4. Bridges, T. M.; LeBois, E. P.; Hopkins, C. R.; Wood, M. R.; Jones, J. K.; Conn, P. J.; Lindsley, C. W. *Drug News & Perspect.* **2010**, *23*, 229.
5. Conn, P. J.; Jones, C.; Lindsley, C. W. *Trends Pharm. Sci.* **2009**, *30*, 148.
6. Yasuda, R. P.; Ciesla, W.; Flores, L. R.; Wall, S. J.; Li, M.; Satkus, S. A.; Weisstein, J. S.; Spagnola, B. V.; Wolfe, B. B. *Mol. Pharmacol.* **1993**, *43*, 149.
7. Wess, J.; Eglen, R. M.; Gautam, D. *Nat. Rev. Drug Disc.* **2007**, *6*, 721.
8. Steidl, S.; Miller, A. D.; Blaha, C. D.; Yeomans *PLoS ONE* **2011**, *6*(11), e27538. http://dx.doi.org/10.1371/journal.pone.0027538.
9. Vilaro, M. T.; Palacios, J. M.; Mengod, G. *Neurosci. Lett.* **1990**, *114*, 154.
10. Weiner, D. M.; Levey, A. I.; Brann, M. R. *Proc. Natl. Acad. Sci. U.S.A.* **1990**, *87*, 7050.
11. Anney, R. J. L.; Lotfi-Miri, M.; Olsson, C. A.; Reid, S. C.; Hemphill, S. A.; Patton, G. C. *BMC Genet.* **2007**, *8*. http://dx.doi.org/10.1186/1471-2156-8-46.
12. Yamada, M.; Lamping, K. G.; Duttaroy, A.; Zhang, W.; Cui, Y.; Bymaster, F. P.; McKinzie, D. L.; Felder, C. C.; Deng, C.-X.; Faraci, F. M.; Wess, J. *Proc. Natl. Acad. Sci. U.S.A.* **2001**, *98*, 14096.
13. Thomsen, M.; Wörtwein, G.; Fink-Jessen, A.; Woldbye, D. P. D.; Wess, J.; Caine, S. B. *Psychopharmacology* **2007**, *192*, 97.
14. Araya, R.; Noguchi, T.; Yuhki, M.; Kitamura, N.; Higuchi, M.; Saido, T. C.; Seki, K.; Itohara, S.; Kawano, M.; Tanemura, K.; Takashima, A.; Yamada, K.; Kondoh, Y.; Kanno, I.; Wess, J.; Yamada, M. *Neurobiol. Dis.* **2006**, *24*, 334.
15. Bridges, T. M.; Marlo, J. E.; Niswender, C. M.; Jones, C. K.; Jadhav, S. B.; Gentry, P. R.; Plumley, H. C.; Weaver, C. D.; Conn, P. J.; Lindsley, C. W. *J. Med. Chem.* **2009**, *52*, 3445.
16. Bridges, T. M.; Kennedy, J. P.; Cho, H. P.; Breininger, M. L.; Gentry, P. R.; Hopkins, C. R.; Conn, P. J.; Lindsley, C. W. *Bioorg. Med. Chem. Lett.* **2010**, *20*, 558.
17. Bridges, T. M.; Kennedy, J. P.; Hopkins, C. R.; Conn, P. J.; Lindsley, C. W. *Bioorg. Med. Chem. Lett.* **2010**, *20*, 5617.
18. Bridges, T. M.; Kennedy, J. P.; Cho, H. P.; Conn, P. J.; Lindsley, C. W. *Bioorg. Med. Chem. Lett.* **2010**, *20*, 1972.
19. Melancon, B. J.; Poslunsey, M. S.; Gentry, P. R.; Tarr, J. C.; Mattmann, M. E.; Bridges, T. M.; Utley, T. J.; Sheffler, D. J.; Daniels, J. S.; Niswender, C. M.; Conn, P. J.; Lindsley, C. W.; Wood, M. R. *Bioorg. Med. Chem. Lett.* **2013**, *23*, 412.
20. Poslunsey, M. S.; Melancon, B. J.; Gentry, P. R.; Bridges, T. M.; Utley, T. J.; Sheffler, D. J.; Daniels, J. S.; Niswender, C. M.; Conn, P. J.; Lindsley, C. W.; Wood, M. R. *Bioorg. Med. Chem. Lett.* **2013**. http://dx.doi.org/10.1016/j.bmcl.2013.01.017.
21. Meshram, H. M.; Ramesh, P.; Kumar, S.; Swetha, A. *Tetrahedron Lett.* **2011**, *52*, 5862.
22. Zhang, J.; Chen, J.; Ding, J.; Liu, M.; Wu, H. *Tetrahedron* **2011**, *67*, 9347.
23. Scheme to access analogs **8** via lithiation/addition sequence.

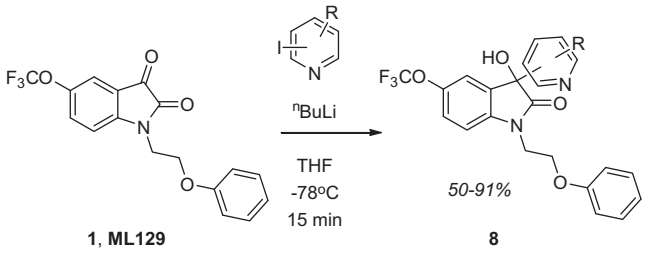

24. Niu, R.; Xiao, J.; Liang, T.; Li, X. *Org. Lett.* **2012**, *14*, 676.
25. Wuitschik, G.; Carreira, E. M.; Wagner, B.; Fischer, H.; Parrilla, I.; Schuler, F.; Rogers-Evans, M.; Muller, K. *J. Med. Chem.* **2010**, *53*, 3227.
26. 1-(2-phenoxyethyl)-5-(trifluoromethoxy)indoline-2,3-dione, ML326: The title compound was synthesized in one step from commercially available starting materials according to the following procedure. Into a 20 mL microwave reaction vial, containing a magnetic stir bar, were weighed 5-(trifluoromethoxy)isatin (460 mg, 2.0 mmol), K_2CO_3 (550 mg, 4.0 mmol), KI (33 mg, 0.20 mmol), followed by acetonitrile (20 mL, 0.1 M) and 2-bromoethyl phenyl ether (480 mg, 2.4 mmol). After being sealed with a crimp cap, the vessel was placed in a microwave reactor and heated to 160 °C for 10 min, with magnetic stirring. After cooling to ambient temperature, the reaction was diluted with CH_2Cl_2 (~20 mL) and washed with brine. The organic layer was separated and dried over Na_2SO_4. Solvent was removed under reduced pressure and the crude product was purified via flash column chromatography (silica gel, hexane/ethyl acetate, 0–50% ethyl acetate gradient). Product containing fractions were combined and the solvents removed under reduced pressure to obtain 583 mg of ML326 (83% yield) as a red-orange powder. TLC R_f = 0.79 (hexane/ethyl acetate 1:1); ^{1}H NMR (400 MHz, $CDCl_3$ calibrated to 7.26) δ 7.52–7.46 (m, 2H), 7.31–7.25 (m, 3H), 6.98 (t, J = 7.4 Hz, 1H), 6.82 (*d*, 2H), 4.28 (t, J = 5.0 Hz, 2H), 4.17 (t, J = 5.0 Hz, 2H); ^{13}C NMR (125 MHz, $CDCl_3$ calibrated to 77.16) δ 182.25, 158.27, 157.93, 150.01, 145.44, 131.02, 129.78, 121.75, 118.32, 114.39, 112.89, 65.94, 40.62; HRMS calcd for $C_{17}H_{13}NO_4F_3$[M+H+]; 352.0797 found: 352.0795.